[CANCER RESEARCH 61, 6592–6600, September 1, 2001]

The Mechanism of the Growth-inhibitory Effect of Coxsackie and Adenovirus Receptor (CAR) on Human Bladder Cancer: A Functional Analysis of CAR Protein Structure[1]

Takatsugu Okegawa, Rey-Chen Pong, Yingming Li, Jeffrey M. Bergelson, Arthur I. Sagalowsky, and Jer-Tsong Hsieh[2]

Department of Urology, The University of Texas Southwestern Medical Center, Dallas, Texas 75390 [T. O., R-C. P., Y. L., A. I. S., J-T. H.], and Division of Immunologic and Infectious Diseases, Children's Hospital of Philadelphia, Philadelphia, Pennsylvania 19104 [J. M. B.]

ABSTRACT

The coxsackie and adenovirus receptor (CAR) is identified as a high-affinity receptor for adenovirus type 5. We observed that invasive bladder cancer specimens had significantly reduced CAR mRNA levels compared with superficial bladder cancer specimens, which suggests that CAR may play a role in the progression of bladder cancer. Elevated CAR expression in the T24 cell line (CAR-negative cells) increased its sensitivity to adenovirus infection and significantly inhibited its *in vitro* growth, accompanied by p21 and hypophosphorylated retinoblastoma accumulation. Conversely, decreased CAR levels in both RT4 and 253J cell lines (CAR-positive cells) promoted their *in vitro* growth. To unveil the mechanism of action of CAR, we showed that the extracellular domain of CAR facilitated intercellular adhesion. Furthermore, interrupting intercellular adhesion of CAR by a specific antibody alleviates the growth-inhibitory effect of CAR. We also demonstrated that both the transmembrane and intracellular domains of CAR were critical for its growth-inhibitory activity. These data indicate that the cell-cell contact initiated by membrane-bound CAR can elicit a negative signal cascade to modulate cell cycle regulators inside the nucleus of bladder cancer cells. Therefore, the presence of CAR cannot only facilitate viral uptake of adenovirus but also inhibit cell growth. These results can be integrated to formulate a new strategy for bladder cancer therapy.

INTRODUCTION

Many studies have explored the potential application of gene therapy on cancer treatment. But a major obstacle of gene therapy is that methods of delivering naked DNA across cell membranes still suffers from low efficiency. Viral entry is mediated by a specific receptor on target cells (1). Recently, a unique transmembrane protein was cloned that is used as a receptor by both coxsackie and adenovirus type 5 (2, 3). Sequence analysis indicates that this CAR[3] cDNA encodes a typical immunoglobulin-like membrane protein with two immunoglobulin domains that interact with adenovirus fiber protein (2–4). Besides its extracellular domain, CAR cDNA contains a 22-amino acid transmembrane domain and a 107-amino acid intracellular domain that has a putative tyrosine phosphorylation site. Its protein structure suggests that CAR may function as more than just a viral receptor, but its biological function is virtually unknown.

In our laboratory, we are evaluating the efficacy of recombinant adenovirus on therapy for human bladder cancer. We observed that a wide spectrum of viral sensitivity among human bladder cancer cell lines correlates with their CAR levels (5). We also found that CAR expression is often down-regulated in cancer specimens but not in adjacent normal tissue. This suggests that altered CAR expression may be involved in the progression of bladder cancer and that decreased CAR levels may result in the poor viral transfection rate in bladder cancer. Therefore, we decided to examine the role of CAR and its structural functional relationship in the biology of bladder cancer and to explore its potential impact on therapy for bladder cancer.

MATERIALS AND METHODS

Cell Culture. All cell lines were obtained from American Type Culture Collection (Manassas, MD) and were grown in T-medium containing 5% fetal bovine serum (5). These cells were routinely cultured in a humidified incubator at 37°C with 5% CO_2.

Tissue Samples. Forty-five patients (36 men and 9 women) received radical cystectomy at the University of Texas Southwestern Medical Center. Mean patient age was 67.3 ± 4.2 years (range, 48–81 years). Cancer stage was assigned according to the Tumor-Node-Metastasis system. Pathological stages of the 45 patients with bladder cancer were: pTis, $n = 4$; pT_1, $n = 4$; pT_2, $n = 9$; pT_3, $n = 13$; pT_4, $n = 3$; pT_xN+, $n = 12$. Normal and cancer tissues derived from the same patient were immediately immersed in liquid nitrogen within 10 min after removal. A portion of each sample was taken for histopathological examination, and the remaining tissue was frozen in liquid nitrogen and stored at −80°C until use. Total cellular RNA was then prepared and subjected to semiquantitative RT-PCR assay.

Sample Collection and Semiquantitative RT-PCR Analysis. For semiquantitative RT-PCR, the assay condition was carried out as described previously (5), which is under linear relationship between PCR product and cDNA levels. Briefly, 2 μg of total cellular from each tissue were reverse transcribed into the first-strand cDNA. One-eighth of the cDNA was subjected to a 20-μl PCR [30 cycles of 92°C (15 s), 55°C (30 s), and 72°C (2 min) using both the CAR primer set (5′-GCCTTCAGGTGCGAGATGTGTTA-3′ and 5′-GAACACGGAGAGCACAGATGAGAC-3′; 0.5 ng/μl) and the GAPDH primer set (5′-TCGTGGAAGGACTCATGACC-3′ and 5′-TCCACCACCCTGTTGCTGTA-3′; 0.5 ng/μl)]. The final PCR products (10 μl) were electrophoresed in a 2% NuSieve agarose gel (3:1 FMC Bioproducts, Rockland, ME) and quantified with BioMax 1D image analysis software (Eastman Kodak, Rochester, NY). The relative level of CAR mRNA from each sample was normalized to GAPDH transcript from the same reaction. We used densitometric analysis to quantify each PCR transcript level. Then, the CAR ratio of tumor *versus* normal from each patient was calculated as CAR (tumor):GAPDH (tumor): CAR (normal):GAPDH (normal).

Plasmid Construction and Transfection into Bladder Cancer Cells. CAR cDNA containing the complete open reading frame was cloned by RT-PCR (5). Two CAR mutants (GPI and Tailless) used in this study were described previously (6). To make another mutant with a complete deletion of the intracellular domain of CAR, the QuikChange Site-Directed Mutagenesis kit was used. Site-directed mutagenesis was performed by PCR according to the manufacturer (Stratagene, La Jolla, CA). The oligonucleotide used for generating two stop codons immediately after the transmembrane domain of Tailless cDNA was 5′-CATTGGTCTTATCATCTTTTGATGATAGTCT-

Received 5/1/01; accepted 6/29/01.

The costs of publication of this article were defrayed in part by the payment of page charges. This article must therefore be hereby marked *advertisement* in accordance with 18 U.S.C. Section 1734 solely to indicate this fact.

[1] This work is supported in part by Grant NIHHL54734 (to J. M. B.).

[2] To whom requests for reprints should be addressed, at Department of Urology, University of Texas Southwestern Medical Center, 5323 Harry Hines Boulevard, Dallas, TX 75390-9110; Phone: (214) 648-3988; Fax: (214) 648-8786; E-mail: JT.Hsieh@UTSouthwestern.edu.

[3] The abbreviations used are: CAR, coxsackie and adenovirus receptor; RT-PCR, reverse transcription-PCR; GAPDH, glyceraldehyde-3-phosphate dehydrogenase; CAM, cell adhesion molecule; FACS, fluorescent-activated cell scanning; AdCMV-β-gal, adenoviral cytomegalovirus-β-galactosidase; GPI, glycosylphosphatidylinositol; Rb, retinoblastoma.

AGA GGGCCCG-3′. Briefly, the denatured Tailless plasmid was reannealed with oligonucleotide primer and subjected to PfuTurbo DNA PCR. After PCR, the methylated and nonmutated parental DNA template was digested with *Dpn*I. The XL-1 Blue cells were then transformed with *Dpn*I-treated DNA for selecting the mutated DNA. Mutants (*i.e.*, Tailless-m) were verified by DNA sequencing. A mammalian expression vector (pcDNA3.1) was used as a plasmid control (Invitrogen, Carlsbad, CA).

To generate an antisense CAR expression vector, pTOPOCAR was digested with *Bam*HI and filled-in. After phenol-chloroform purification, this CAR insert was isolated after *Eco*RI digestion. The insert was then subcloned into both *Sma*I and *Eco*RI sites of pCI-neo (Promega, Madison, WI).

To generate stable transfectants, both T24 and 253J cells (2×10^5 per p-35 plate) were transfected with 2 μg of cDNA using Lipofectamine transfection reagent (Life Technologies, Rockville, MD). For RT4 cells, 2.5×10^6 (per p-100 plate) cells were transfected with 10 μg of cDNA using electroporation. Cells were selected for neomycin-resistant clones with G-418 (600 μg/ml) 48 h after transfection. Resistant colonies were cloned by ring isolation 2 weeks after selection.

Determination of CAR Levels by FACS. Cytometric analysis was used to determine CAR levels for each clone. Briefly, membrane fluorescence staining was performed on a single-cell suspension using RmcB monoclonal antibody and FITC-conjugated secondary antibodies (5, 7). Fluorescence-activated cell scanning was performed with a dual-laser Vantage flow cytometer (Becton Dickinson, Mountain View, CA), which delivered 50 mW at 488 nm with an Enterprise air-cooled laser. Analysis was performed using LYSYS II software (Becton Dickinson, Mountain View, CA). The positive population of cells was determined by gating the right-hand tail of the distribution of the negative control sample for each individual cell line at 1% as described previously (5, 7). This setting was then used to determine the percentage of positive cells for each of the above markers for each individual cell line.

Detection of Virus-mediated Gene Delivery. To determine the viral sensitivity of human bladder cancer cells, 5×10^5 cells were infected with different concentrations of AdCMV-β-gal at 37°C (8). Twenty-four h after infection, the β-gal activity was measured in a 200-μl cell lysate and normalized to the protein concentration of each sample.

Determination of *in Vitro* Growth Rate of CAR-transfected Bladder Cancer Cell Line. To examine the effect of CAR on the cell growth, cells were plated at a density of 5000 cells in 48-well plates with T-medium containing 0.2% fetal bovine serum. Relative cell numbers were determined by crystal violet assay (9, 10) at the indicated time.

Western Analysis of p21 and pRb Expression. To examine the p21 and Rb protein levels in each transfectant, we performed Western blot analysis (11). The cell lysate was prepared by adding 20% SDS containing 1 mM phenylmethylsulfonyl fluoride. The lysate was sonicated for 30 s on ice, followed by centrifugation for 5 min at 4°C. Twenty μg of total protein from each sample were subjected to a 10% SDS-polyacrylamide gel and electrotransferred to a nitrocellulose membrane. After blocking with PBS containing 5% powdered milk, the membrane was incubated with either anti-p21 (6B6; PharMingen, San Diego, CA) or anti-Rb (G3–245; PharMingen) antibody for 1 h, followed by incubation with antimouse IgG. After extensive washing, the protein was visualized with an ECL-chemiluminescence detection kit (Amersham, Arlington Heights, IL).

Cell Adhesion Assay. Cells were trypsinized into a signal cell suspension at a concentration of 1×10^6 cells/ml. Cell suspension (1 ml) in a 1.5-ml Eppendorf tube was mixed gently at room temperature to allow cell aggregates to form. Samples were taken over a 5-h period, and the number of single cells was determined using a hemacytometer. The degree of cell adhesion was represented as a decrease in the percentage of single cells (12).

Statistical Analysis. All data were evaluated using Student's *t* test. Probability values less than 0.05 or 0.01 were considered significant.

RESULTS

Decreased CAR mRNA in Human Bladder Cancer Specimens. Loss or decreased CAR expression is detected in several human bladder cancer cell lines (5). We decided to investigate whether altered CAR expression is also present in human bladder cancer specimens. As shown in Fig. 1*A*, using semiquantitative RT-PCR

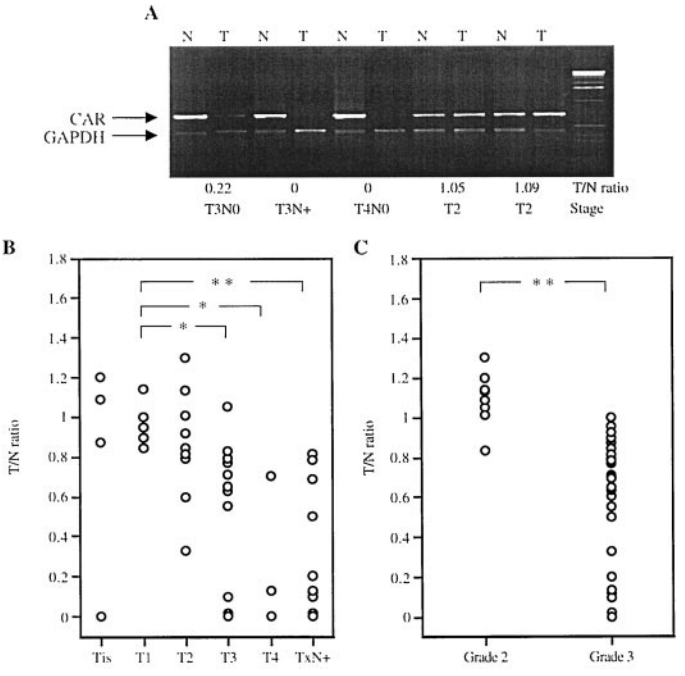

Fig. 1. Determination of CAR expression in bladder cancer specimens using quantitative RT-PCR assay. *A*, the profile of CAR expression from a paired sample derived from the same patient. Total cellular RNAs prepared from each paired specimen were subjected to semiquantitative RT-PCR analysis. *B*, the T:N ratio of CAR levels from different pathological stages of bladder cancer patients. *C*, the T:N ratio of CAR levels from different grades of bladder cancer patients. *N*, normal; *T*, tumor. *, significantly different from pT_1 ($P < 0.05$); **, significantly different from pT_1 ($P < 0.01$).

assay, a wide spectrum of CAR mRNA expression was detected. However, we observed that all of the normal tissue expressed detectable levels of CAR mRNA. As shown in Fig. 1*B*, the CAR levels in specimens obtained from pT_1 (0.96 ± 0.11) and pT_2 (0.85 ± 0.26) are similar. However, based on the pathological feature of each specimen, the mean values of T:N ratio of CAR in pT_3, pT_4, or pT_xN+ were significantly lower than values in pT_1 ($P < 0.05$). Furthermore, the T:N ratio of CAR in specimens with grade 3 tumor is significant lower than grade 2 tumor (Fig. 1*C*). These data indicate that decreased expression of CAR is often associated with high grade and/or stage of human bladder cancer.

Correlation between CAR Levels and Viral Sensitivity of Human Bladder Cancer. Cytometric analysis of membrane CAR expression of human bladder cancer cell lines (T24, 253J, and RT4) indicated that 253J and RT4 contained 95 and 96% CAR-positive cells, respectively, whereas T24 contained only 13% CAR-positive cells. The viral sensitivity of each cell line correlated with the percentage of CAR-positive cells (Table 1) as determined by AdCMV-β-gal.

As shown in Fig. 2*A*, CAR appears to be a typical immunoglobulin-like protein containing extracellular, transmembrane, and intracellular domains. To determine which domain is crucial for adenoviral infection in human bladder cancer cells, we transfected a series of CAR expression vectors into T24 cells, including GPI, Tailless, and Tailless-m (Fig. 2*A*). GPI cDNA contains only the extracellular domain of CAR with an additional glycolipid anchor domain for membrane attachment. Tailless cDNA contains the extracellular domain, transmembrane domain, and the first two amino acids from the intracellular domain of CAR. Tailless-m cDNA contains both the extracellular and transmembrane domains. For T24 cells, two independent CAR clones (T24-CAR3 and T24-CAR4), one plasmid control (T24-vector) and six independent clones of CAR mutants (T24-GPI13, T24-GPI24, T24-Tailless1, T24-Tailless7, T24-Tailless-m1, and T24-Tailless-m2)

Table 1 *Correlation between CAR levels and virus sensitivity of bladder cancer cells*

Cell line	FACS (%)[a]	β-gal activity ($A_{405\ nm}/\mu g$)[b]		
		Control	10 MOI	100 MOI
T24-parental	13	0.68 ± 0.24	2.23 ± 0.72	7.9 ± 1.0
T24-vector	4	0.78 ± 0.38	1.55 ± 0.01	3.9 ± 0.5
T24-CAR2	61	0.98 ± 0.24	19.22 ± 1.61	107.5 ± 7.7
T24-CAR3	45	0.87 ± 0.63	6.72 ± 0.38	31.8 ± 3.4
T24-GPI10	47	1.01 ± 0.36	6.99 ± 0.20	28.6 ± 1.9
T24-GPI13	59	0.87 ± 0.54	7.01 ± 1.21	33.6 ± 0.8
T24-GPI24	20	0.96 ± 0.24	3.01 ± 0.28	21.0 ± 1.9
T24-Tailless1	95	0.59 ± 0.02	25.38 ± 3.63	166.2 ± 4.5
T24-Tailless7	64	0.83 ± 0.06	10.87 ± 1.88	86.8 ± 2.7
T24-Tailless-m1	83	0.89 ± 0.08	21.54 ± 1.23	147.5 ± 3.8
T24-Tailless-m2	67	0.58 ± 0.14	11.05 ± 0.87	110.3 ± 7.6
253J-parental	95	0.91 ± 0.25	18.89 ± 0.36	197.6 ± 3.5
253J-vector2	90	0.83 ± 0.54	17.01 ± 0.91	189.4 ± 3.4
253J-vector3	92	0.93 ± 0.25	21.01 ± 0.35	186.0 ± 4.9
253J-antiCAR3	43	0.58 ± 0.03	11.42 ± 0.46	36.2 ± 4.5
253J-antiCAR10	13	0.98 ± 0.26	7.42 ± 0.35	19.6 ± 2.3
253J-antiCAR12	28	0.82 ± 0.08	10.81 ± 0.85	36.3 ± 3.4
RT4-parental	96	0.54 ± 0.12	19.02 ± 0.21	194.4 ± 3.8
RT4-vector1	92	0.61 ± 0.26	18.25 ± 0.28	190.3 ± 4.1
RT4-vector2	95	0.73 ± 0.45	20.33 ± 0.32	196.6 ± 5.7
RT4-antiCAR1	23	0.98 ± 0.24	3.25 ± 0.36	21.5 ± 1.5
RT4-antiCAR3	46	0.65 ± 0.13	10.76 ± 0.42	41.2 ± 2.5

[a] Cells were incubated with RmcB monoclonal antibody before the addition of FITC-conjugated antimouse IgG secondary antibody. Data are calculated as described in "Materials and Methods" and presented as the percentage of cells gated positive. MOI, multiplicity of infection.

[b] Each value was determined in triplicate from two separate experiments.

were selected according to different plasmid DNA integration patterns (data not shown).

On the other hand, we transfected an antisense CAR vector into both 253J and RT4 cells. For 253J, three independent antisense CAR clones (253J-antiCAR3, 253J-antiCAR10, and 253J-antiCAR12) and two plasmid controls (253J-vector2 and 253J-vector3) were selected. For RT4, two independent antisense CAR clones (RT4-antiCAR1 and RT4-antiCAR3) and two plasmid controls (RT4-vector1 and RT4-vector2) were selected.

Cytometric analysis of the transfected bladder cancer cells using CAR monoclonal antibody (RmcB) was performed 1 month after G-418 selection. As shown in Table 1, the amount of CAR-positive cells in T24-CAR2 or CAR3 was 61 and 45%, respectively. In contrast, the amount of CAR-positive cells in the T24-vector clone was ~4%. Cytometric analysis revealed that the CAR-positive cell population was enriched approximately 10- to 15-fold compared with T24-vector cells. In contrast, the CAR- positive cells in antisense CAR-transfected 253J and RT4 clones were decreased (ranging from 50 to 85%) compared with either parental or vector cells. Results obtained from β-gal activity elicited by AdCMV-β-gal indicated that the β-gal activity paralleled CAR levels from each clone.

However, three different CAR mutants (*i.e.,* GPI, Tailless, and Tailless-m) were still sensitive to adenovirus, which indicates that the extracellular domain of the CAR protein is critical for virus binding (Table 1). However, we observed a slight decrease of β-gal in both T24-GPI10 and T24-GPI13 cells without transmembrane domain of CAR, suggesting that the transmembrane domain may also contribute to virus internalization. Nevertheless, these data indicate that viral sensitivities of bladder cancer cell lines correlate with their CAR levels.

Cell Adhesion Activity of the CAR Protein. Because CAR is structurally similar to the immunoglobulin-superfamily CAM, we thought it important to determine whether CAR behaves like an

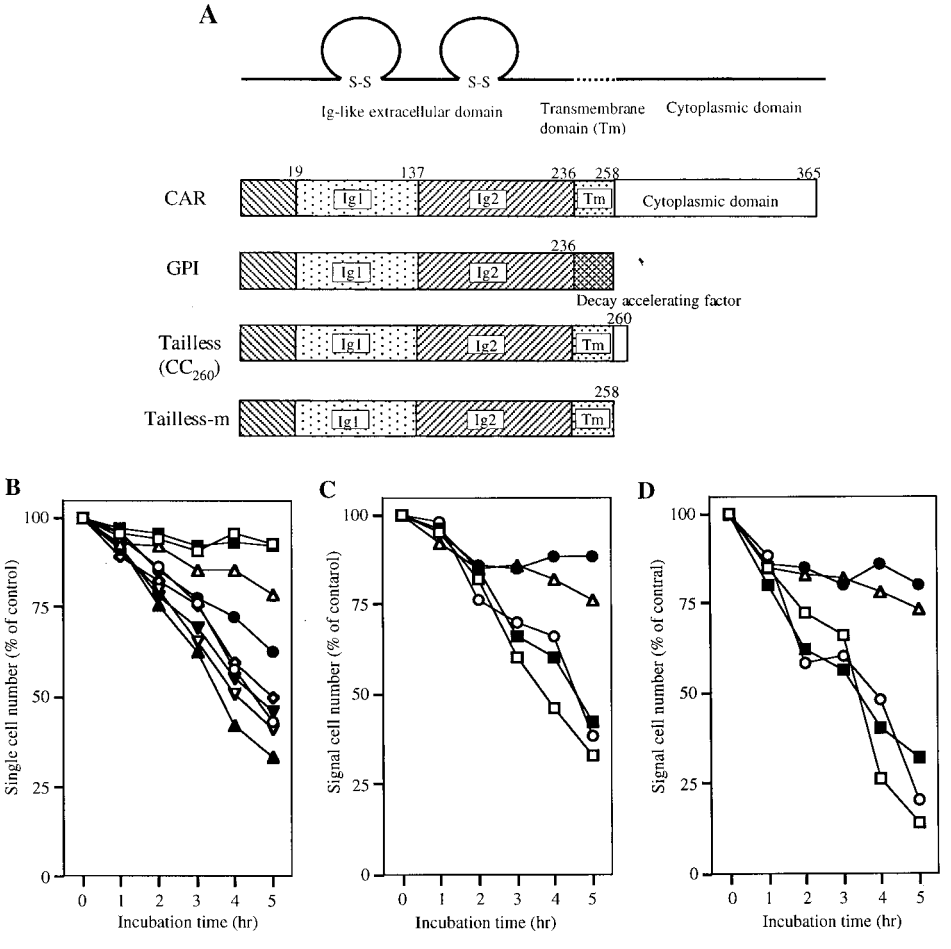

Fig. 2. Increased cell adhesion activity in CAR-expressing bladder cancer cells. *A,* schematic representation of the CAR molecule and CAR mutants. The wild-type CAR protein contains 365 amino acids. GPI contains an extracellular domain fused with the 37 COOH-terminal amino acids of the human decay-accelerating factor with glycolipid anchor ability. Tailless contains immunoglobulin extracellular domain, transmembrane domain, and the first two amino acids of intracellular domain. Tailless-m contains both extracellular domain and transmembrane domain. *B–D,* cell adhesion assay. Single-cell suspension was prepared by trypsin digestion of cells from tissue culture plate. One million cells were incubated at room temperature with constant mixing. At the indicated time, an equal volume of cell suspension was collected, and the number of single cells was counted with a hemacytometer. Each point represents the mean value averaged from samples in triplicate, and the SE is <10% of the mean. *B,* T24-parental (□), T24-vector (■), T24-CAR2 (○), T24-GPI13 (●), T24-GPI24 (△), T24-Tailless1 (▲), T24-Tailless7 (▽), T24-Tailless-m1 (▼), T24-Tailless-m2 (◇). *C,* 253J-parental (□), 253J-vector2 (■), 253J-vector3 (○), 253J-antiCAR10 (●), 253J-antiCAR12 (△). *D,* RT4-parental (□), RT4-vector1 (■), RT4-vector2 (○), RT4-antiCAR1 (●), and RT4-antiCAR3 (△).

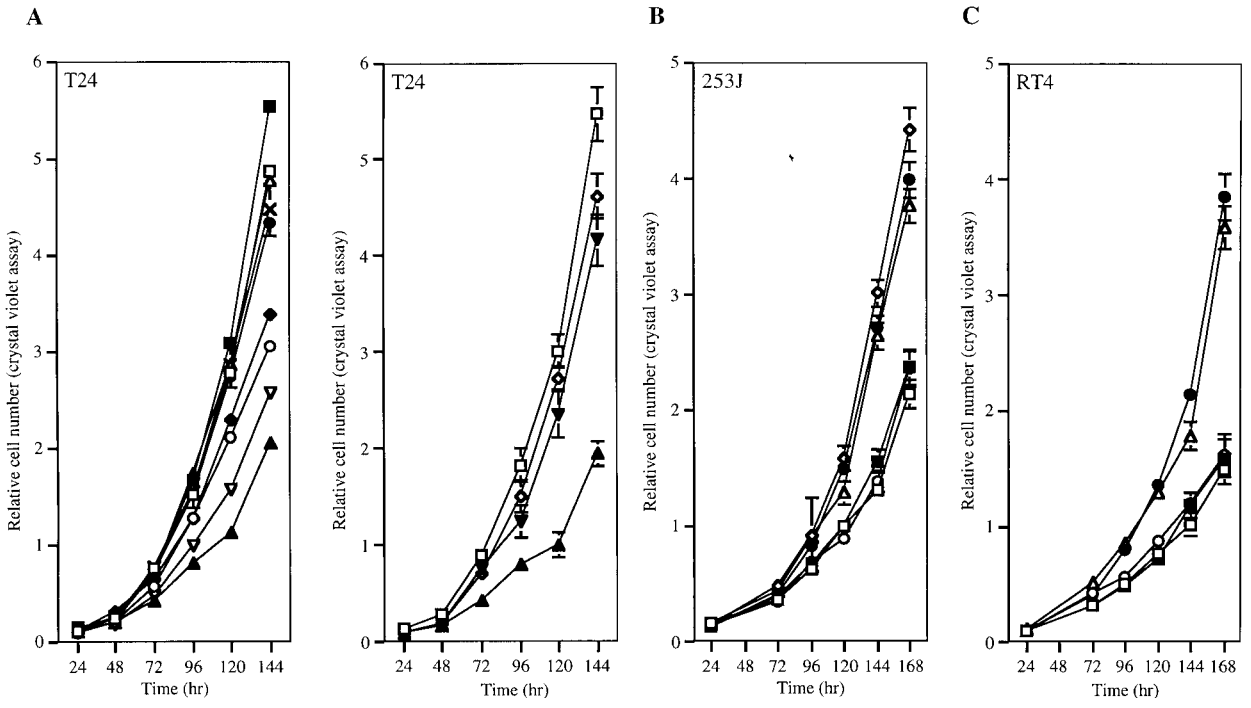

Fig. 3. The impact of CAR on *in vitro* growth rate of bladder cancer cells. *A*, T24-parental (□); T24-vector (■); T24-CAR2 (○); T24-CAR3 (♦); T24-GPI10 (×); T24-GPI13 (●); T24-GPI24 (△); T24-Tailless1 (▲); T24-Tailless7 (▽); T24-Tailless-m1 (▼); T24-Tailless-m2 (◇). *B*, 253J-parental (□); 253J-vector2 (■); 253J- vector3 (○); 253J-antiCAR3 (●); 253J-antiCAR10 (◇); 253J-antiCAR12 (△). *C*, RT4-parental (□); RT4-vector1 (■); RT4-vector2 (○); RT4-antiCAR1 (●); RT4-antiCAR3 (△). *Bars*, SE.

adhesion molecule. To do this, the time course of aggregate formation for all of the transfectants was examined. As shown in Fig. 2*B*, T24-parental and T24-vector cells, both with low levels of CAR, formed few aggregates during the 5-h incubation period. Generally, all of the CAR-transfected T24 clones formed aggregates in a time-dependent manner. The extent of aggregation appeared to correlate well with the level of CAR expression on each subline. Conversely, the antisense CAR-transfected 253J and RT4 cells with lower levels of CAR formed few aggregates compared with their parental and plasmid control cells (Fig. 2, *C* and *D*). We also noticed that T24-GPI13 and T24-GPI14 formed less aggregate than other sublines, suggesting that the transmembrane form of CAR molecule has the better ability to stabilize the cell-cell interaction between bladder cells.

***In Vitro* Growth Characteristics of CAR-transfected Bladder Cancer Cells.** Cell adhesion molecules such as C-CAM1 play an important role in suppressing the progression of both prostate and bladder cancers (12–15). Also, the increased CAR expression can inhibit both *in vitro* and *in vivo* growth of human prostate cancer cell lines (PC-3; Ref. 7). Therefore, we decided to examine the effect of CAR on the *in vitro* growth rate of bladder cell line cells. Compared with either T24-parental or T24-vector cells, the growth rate of T24-CAR2 and T24-CAR3 cells decreased approximately 43 and 30%, respectively, at day 6 (Fig. 3*A*). Because our data indicated that the extracellular domain of CAR is critical for viral uptake (Table 1), we further examined the structural functional relationship between the CAR domains and its growth-inhibitory activity. Two Tailless sublines (*i.e.,* T24-Tailless1 and Tailless7) grew even slower than T24-CAR2 or T24-CAR3 cells *in vitro* (Fig. 3, *A* and *B*). This higher degree of growth inhibition elicited by the Tailless cDNA may be attributable to the higher levels of CAR expression from each subline (Table 1 and Fig. 3*A*). For example, the growth rate of T24-Tailless1 and T24-Tailless cells decreased approximately 64 and 55% compared with T24-vector cells, respectively, at day 6 (Fig. 3*A*). In contrast, two GPI sublines (*i.e.,* T24-GPI10 and GPI13) did not exhibit any growth inhibition (Fig. 3*A*), although these sublines expressed similar CAR levels as T24-CAR2 cells. Furthermore, both T24-Tailless-m1 and T24-Tailless-m2 cells did not exhibit any growth inhibition (Fig. 3*A*), although both sublines have a high percentage of CAR-positive cells, which suggests that the first two amino acids in the intracellular domains of CAR are critical for its tumor-inhibitory activity. These data indicate that CAR can act as a membrane receptor to elicit the growth-inhibitory signal in bladder cancer cells.

The growth rate of three antisense CAR-transfected 253J cells increased almost 2-fold compared with both 253J-parental and 253J-vector cells at day 7 (Fig. 3*B*). Similarly, the growth rate of two antisense CAR-transfected RT4 cells also increased 2.5-fold compared with both RT4-parental and RT4-vector cells at day 7 (Fig. 3*C*). These finding indicate clearly that CAR is a potent growth inhibitor for bladder cancer cells.

Moreover, Western blot analyses (Fig. 4, *A* and *B*) provided direct evidence that p21 levels increased in T24-CAR2, T24-Tailless1, and T24-Tailless7 cells in a time-dependent manner, whereas the growing cells (such as T24-parental, T24-vector control, T24–GPI, and T24-Tailless-m cells) had very low p21 proteins. Similarly, the steady-state levels of Rb protein, a key effector for p21-induced grow inhibition, were substantially reduced in T24-CAR2, T24-Tailless1, and T24-Tailless7. Also, the majority of Rb protein was hypophosphorylated in these three sublines (Fig. 4*A*). In contrast, hyperphosphorylated Rb protein was associated with the growing cells (such as T24-parental, T24-vector control, T24–GPI, and T24-Tailless-m cells; Fig. 4, *A* and *B*).

As shown in Fig. 3, *B* and *C*, antagonizing endogenous CAR levels in either 253J or RT4 cells led to a higher *in vitro* growth rate. This was evidenced by decreased p21 levels and increased hypophosphorylated Rb levels in these sublines. These data suggest that CAR is able to elicit the growth-inhibitory signals, such as p21 and Rb, to modulate cell cycle regulators inside the nucleus of bladder cancer cells.

Effect of Adhesion Activity of CAR on Growth Inhibition of Bladder Cancer Cells. To examine the specificity of the intercellular adhesion mediated through the CAR molecule, we tested whether

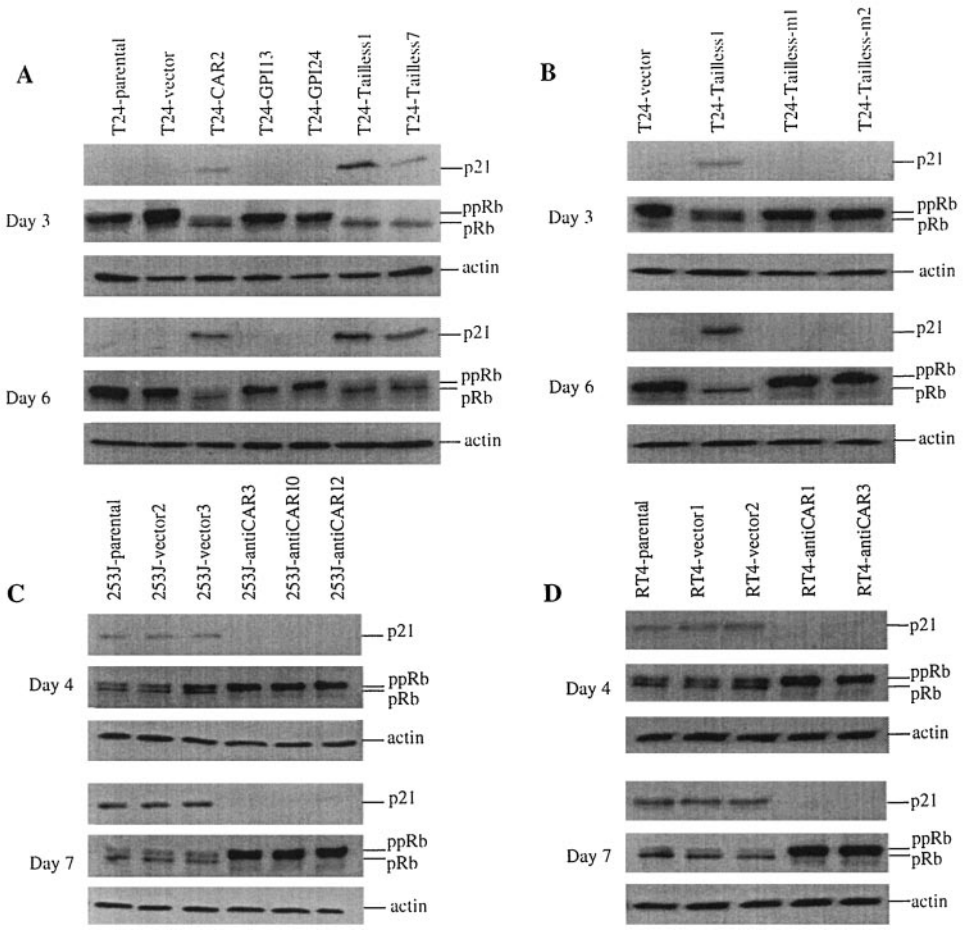

Fig. 4. The effect of CAR on the expression of p21 and Rb protein in bladder cancer cells. At the indicated time, cell lysates from T24 sublines (*A* and *B*), 253J sublines (*C*), and RT4 sublines (*D*) were subjected to Western blot analysis probed with anti-p21, Rb, and β-actin antibodies. *ppRb*, hyperphosphorylated form of Rb; *pRb*, hypophosphorylated form.

RmcB monoclonal antibody (2) can block intercellular adhesion. Aggregates formed by T24-CAR2, T24-GPI, T24-Tailless, and T24-Tailless-m sublines can be inhibited in the presence of the RmcB monoclonal antibody (Fig. 5, *B–H*). However, T24-parental cells were not inhibited under the same experimental condition because this line did not form cell aggregates (Fig. 5*A*). Moreover, aggregates formed by 253J-parental and RT4-parental cells can be partially blocked by RmcB monoclonal antibody (Fig. 5, *I* and *J*). Noticeably, this inhibition proceeded in a dose-dependent manner. For example, RmcB with 1:10 dilution had greater inhibitory activity than two other dilutions (1:100 or 1:2500). We used an antibody (Chemicon, Inc., Temecula, CA) against integrin $\alpha_v\beta_5$ as the control antibody because $\alpha_v\beta_5$ levels in T24, 253J, and RT4 cells were 85.3, 88.9, and 1.7%, respectively. Nevertheless, the presence of control antibody failed to impede cell aggregation. These results indicate that the aggregation of CAR-positive cells can be mediated through CAR proteins.

We further examined the impact of cell aggregation on the growth rate of CAR-transfected cells. Eight different CAR-transfected T24 sublines were incubated with RmcB monoclonal antibody with 1:10 dilution. Then, total cell number was determined at the indicated time (Fig. 6). In the presence of RmcB antibody, the growth rate of T24-parental, T24-GPI13, T24-GPI24 cells, T24-Tailless-m1, and T24-Tailless-m2 did not change (Fig. 6, *A*, *C*, *D*, *G*, and *H*), suggesting that the intracellular domain of CAR is required for its growth suppression. However, the growth rate of T24-CAR2, T24-Tailless1, and T24-Tailless7 cells increased in the presence of RmcB antibody (Fig. 6, *B*, *E*, and *F*). Similarly, the RmcB antibody was able to enhance the growth rate of 253J- and RT4-parental cells (Fig. 6, *I* and *J*). Moreover, as shown in Table 2, the neutralizing effect of RmcB antibody on the *in vitro* growth inhibition of CAR-positive cells proceeded in a dose-dependent manner. In all experiments, the control antibody (anti-integrin $\alpha_v\beta_5$) did not have any effect on CAR-transfected cells. These data indicate that the growth inhibition of bladder cancer cells can be mediated by the cell adhesion activity of CAR proteins.

We also examined the levels of expression of p21 and Rb protein in CAR-transfected T24 sublines treated with RmcB antibody (Fig. 7*A*). Apparently, treatment of RmcB antibody can stimulate the growth rate of T24-CAR2 and T24-Tailless1 cells that were accompanied with the decreased p21 levels and increased hyperphosphorylated Rb levels in these cells. RmcB did not completely suppress the p21 and Rb levels in T24-Tailless1, which may be attributable to the very higher CAR expression in these sublines. Also, RmcB antibody failed to block the cell growth of T24-Tailless-m sublines. This was evidenced by no elevation of either p21 or hypophosphorylated Rb levels (Fig. 6, *G* and *H*, and Fig. 7*A*). Furthermore, RmcB antibody can restore the growth rate of 253J- and RT4-parental cells, which was reflected by the decreased p21 levels and the increased hyperphosphorylated Rb levels in these cells (Fig. 7*B*). These data indicate that interruption of CAR interaction is critical for blocking the transduction of the growth-inhibitory signal into the nucleus of bladder cancer cells.

DISCUSSION

Genetic alteration is a major cause of malignant transformation and cancer progression. Gene therapy is based upon the idea that replacing absent critical functional gene(s) in target cells can alter the malignant phenotype. Adenoviral entry into target cells is the rate-limiting step

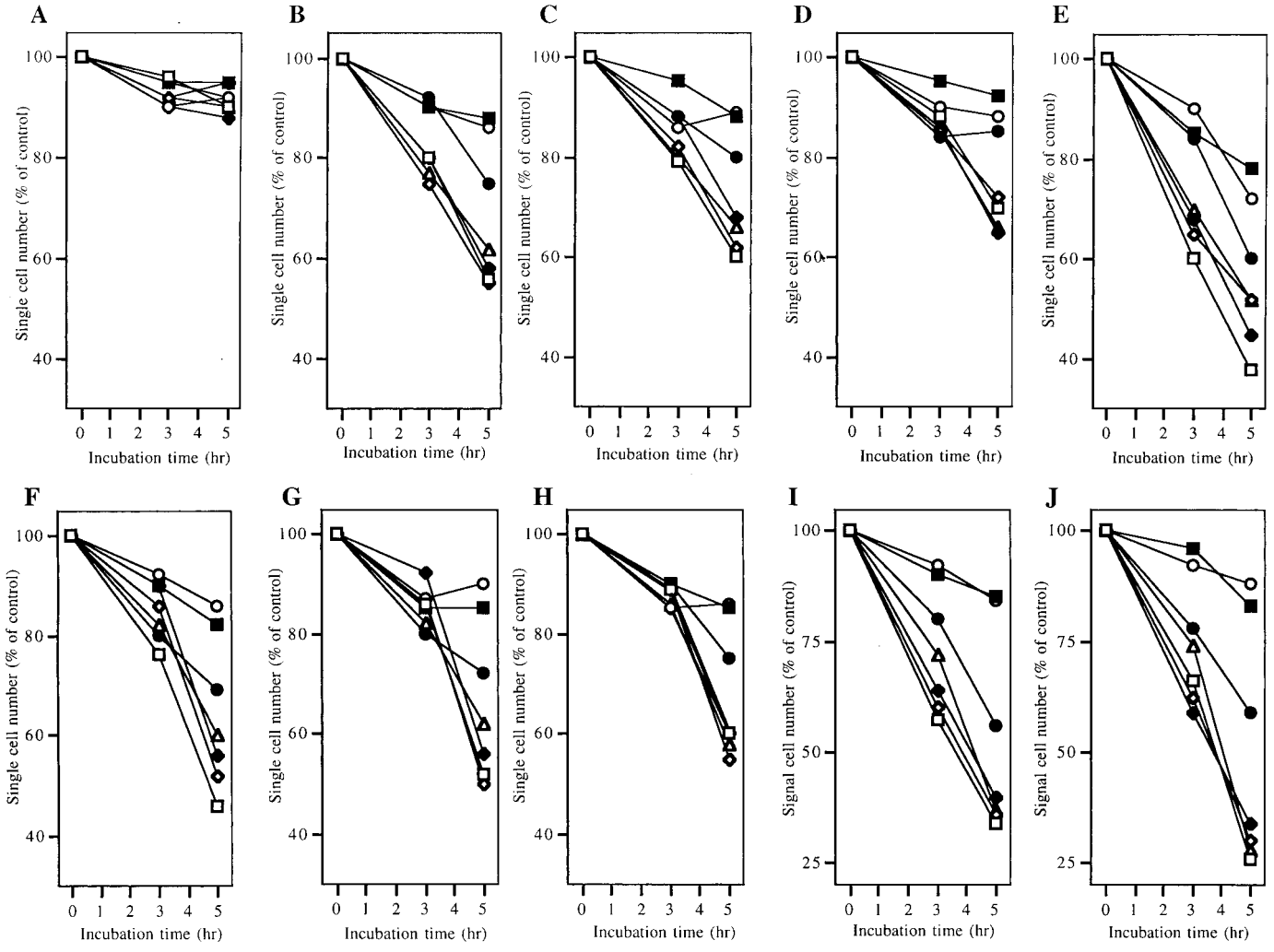

Fig. 5. The effect of CAR antibody on cell adhesion of bladder cancer cells. Single-cell suspension (*A*, T24-parental; *B*, T24-CAR2; *C*, T24-GPI13; *D*, T24-GPI24; *E*, T24-Tailless1; *F*, T24-Tailless7; *G*, T24-Tailless-m1; *H*, T24-Tailless-m2; *I*, 253J; *J*, RT4) was prepared by trypsin digestion of cells from tissue culture plate. One million cells were incubated at room temperature with various concentrations of RmcB monoclonal antibody. At the indicated time, an equal volume of cell suspension was collected, and the number of single cells was counted with a hemacytometer. □, no antibody; ■, 1:10 RmcB; ○, 1:100 RmcB; ●, 1:2500 RmcB; ◇, 1:10-anti-integrin $\alpha_v\beta_5$; ◆, 1:100-anti-integrin $\alpha_v\beta_5$; △, 1:2500-anti-integrin $\alpha_v\beta_5$.

of gene delivery. The recombinant adenovirus, in contrast to other vectors available for gene therapy, is highly infectious and capable of transferring transgenes into nondividing cells (16). This vector system appears to be suitable for bladder cancer that has a heterogeneous mitotic pattern. The initial binding of adenovirus to the cell surface is a receptor-mediated process (17, 18), and the adenovirus fiber protein is responsible for attachment of the virus to the cellular receptor. CAR was identified recently as a high-affinity receptor for adenovirus (2, 3).

With both receptor binding and virus infectivity assays, we found that the levels of CAR correlate with the viral sensitivity of each cell line determined. To reverse viral resistance of T24 cells, we genetically engineered T24 cells by increasing CAR-positive cells to 61% (T24-CAR2) or to 45% (T24-CAR3). Transgene activity in CAR-positive cells such as β-gal increased about 10- to 30-fold compared with the control cells (Table 1). Because a lower dose of adenovirus delivery into CAR-positive cells can achieve the same therapeutic outcome as a higher dose, careful determination of CAR status in target tissue must be evaluated prior to gene therapy trials to avoid undesirable cytotoxicity or immune response caused by excessive administration of adenovirus.

Recently, we reported that a wide spectrum of CAR levels exists among several human bladder cancer lines (4). Similar reports confirm this observation in other cancer types such as melanoma and glioma (19–21). With Northern blot and semiquantitative RT-PCR analyses, we documented that a significant difference in viral receptor levels is caused by down-regulation of the *CAR* gene in several resistant cancer cell lines. We also found that bladder cancer specimens from pT_3, pT_4, or pT_xN+ had significantly reduced levels of CAR mRNA compared with those from either pT_1 or pT_2 (Fig. 1*B*). Also, bladder cancer with high grade expressed less CAR mRNA than cancer with low grade (Fig. 1*C*). This finding has several significant implications regarding the impact of CAR status on the efficacy of gene therapy trials for human bladder cancer and on the biological role of CAR in disease progression.

We noticed that CAR-transfected T24 cells showed increased cell aggregation compared with either the T24-parental or the T24-vector cells, which indicates that CAR is a typical CAM (Fig. 2). We also observed a similar degree of cell aggregation from T24-GPI, T24-Tailless, and T24-Tailless-m sublines. In addition, the CAR-specific antibody is also able to interrupt the cell aggregation of these sublines (Fig. 5). Therefore, these data indicate that the extracellular domain of CAR has an adhesion activity. We observed decreased cell aggregation in antisense CAR-transfected 253J and RT4 sublines compared

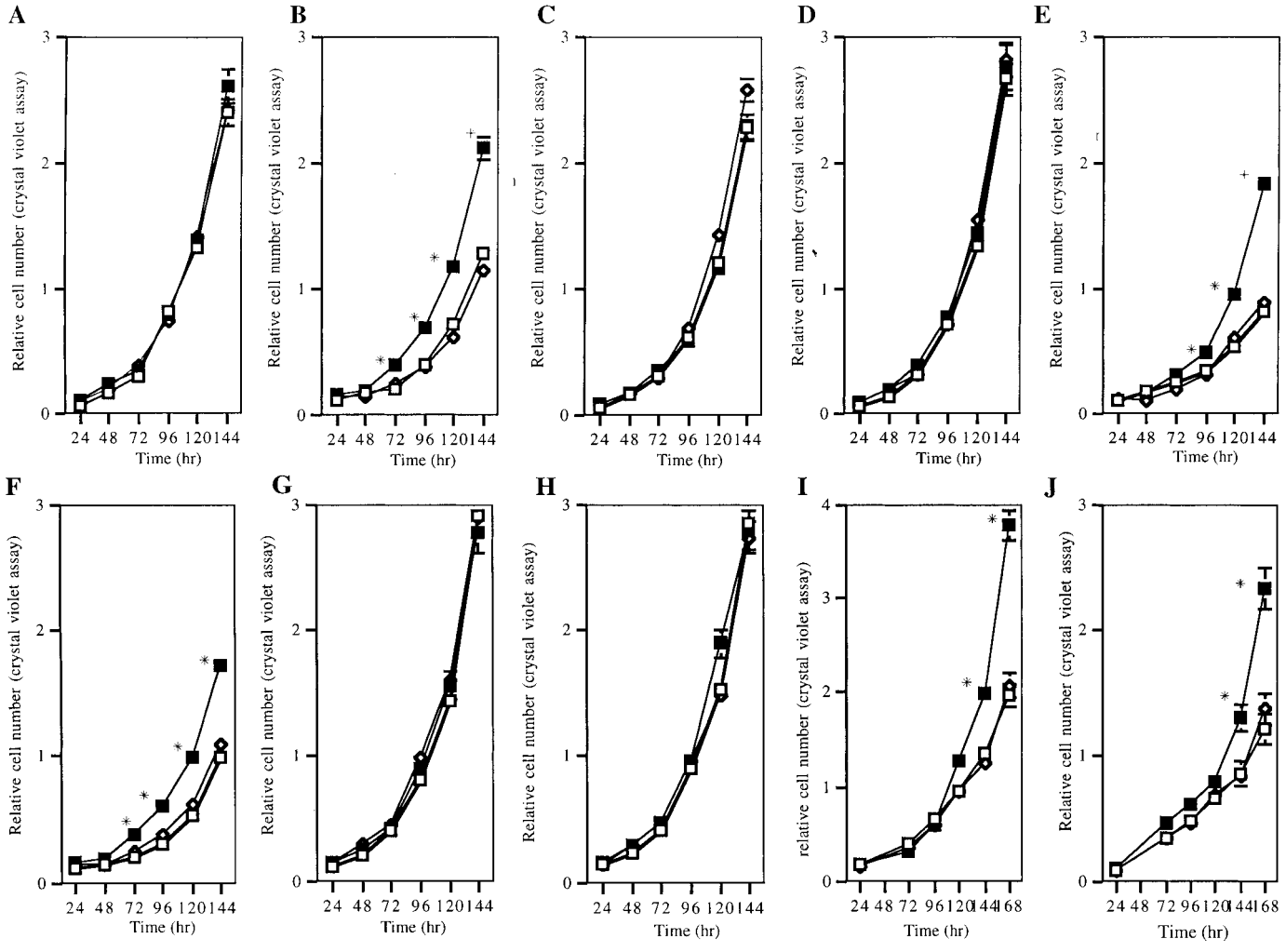

Fig. 6. The effect of CAR antibody on the growth of bladder cancer cells. Cells (*A*, T24-parental; *B*, T24-CAR2; *C*, T24-GPI13; *D*, T24–24; *E*, T24-Tailless1; *F*, T24-Tailless7; *G*, T24-Tailless-m1; *H*, T24-Tailless-m2; *I*, 253J; *J*, RT4) were plated at a density of 5000 cells/ml in 48-well plates incubated with either 1:10 RmcB monoclonal antibody or 1:10 anti-integrin. Cells were harvested and counted at the indicated time. □, no antibody; ■, 1:10 RmcB; ◇, 1:10 anti-integrin $\alpha_v\beta_5$. *, significantly different from no antibody ($P < 0.01$). *Bars*, SE.

with their parental or vector cells. Honda *et al.* (22) report that CAR has the intercellular adhesion activity in the developing mouse brain, which suggests that CAR may mediate cell-cell recognition during brain development. Taken together, we believe that cell adhesion activity of CAR may play a potential role in both bladder and brain biology.

To determine which CAR functional domain is responsible for its tumor-inhibitory activity, CAR deletion mutants in T24 cells were examined using *in vitro* growth tumorigenicity assay. CAR from which all but two cytoplasmic domain residues had been deleted still retained its tumor-inhibitory activities; CAR lacking the entire cytoplasmic domain or CAR lacking both transmembrane and cytoplasmic domains did not (Fig. 3*A*). This indicates that both the transmembrane domain and the first two amino acids (*i.e.*, cysteine-cysteine) in the intracellular domain of CAR are critical for growth inhibition in bladder cancer cells. The cysteine residues in the intracellular domain

Table 2 *Effect of the CAR antibody on the growth of bladder cancer cells*[a]

Cell line	Control[b]	RmcB[c] 1:2500	RmcB[c] 1:1000	RmcB[c] 1:100	RmcB[c] 1:10	Integrin[c] 1:10
T24-parental	2.42 ± 0.05	2.46 ± 0.07	2.49 ± 0.09	2.48 ± 0.07	2.51 ± 0.09	2.43 ± 0.07
T24-CAR2	1.79 ± 0.06	1.71 ± 0.07	1.92 ± 0.06[d]	2.44 ± 0.03[d]	2.62 ± 0.02[d]	1.77 ± 0.05
T24-GPI13	2.21 ± 0.04	2.23 ± 0.09	2.32 ± 0.02	2.20 ± 0.05	2.30 ± 0.08	2.19 ± 0.02
T24-GPI24	2.61 ± 0.01	2.60 ± 0.06	2.65 ± 0.06	2.54 ± 0.05	2.70 ± 0.04	2.66 ± 0.04
T24-Tailless1	1.20 ± 0.09	1.30 ± 0.02	1.65 ± 0.04[d]	1.96 ± 0.03[d]	2.37 ± 0.03[d]	1.32 ± 0.07
T24-Tailless7	1.37 ± 0.08	1.41 ± 0.02	1.85 ± 0.04[d]	2.04 ± 0.02[d]	2.46 ± 0.07[d]	1.43 ± 0.02
T24-Tailless-m1	2.45 ± 0.05	2.36 ± 0.06	2.43 ± 0.02	2.21 ± 0.07	2.33 ± 0.05	2.39 ± 0.08
T24-Tailless-m2	2.33 ± 0.07	2.24 ± 0.08	2.29 ± 0.05	2.38 ± 0.09	2.29 ± 0.08	2.39 ± 0.05
253J-parental[b]	2.01 ± 0.07	2.10 ± 0.09	2.62 ± 0.09[d]	2.96 ± 0.11[d]	3.21 ± 0.10[d]	1.99 ± 0.06
RT4-parental[b]	1.13 ± 0.09	1.19 ± 0.08	1.61 ± 0.02[d]	1.91 ± 0.09[d]	2.19 ± 0.11[d]	1.02 ± 0.03

[a] Cells were plated at a density of 5000 cells/ml in 48-well plates in T-medium containing 0.2% FBS. Cells were harvested at day 6 and counted by crystal violet assay.
[b] 253J and RT4 cells were harvested at day 7 and counted by crystal violet assay.
[c] Relative cell number (mean ± SD).
[d] The test is significant compared with control ($P < 0.01$) by Student's *t* test.

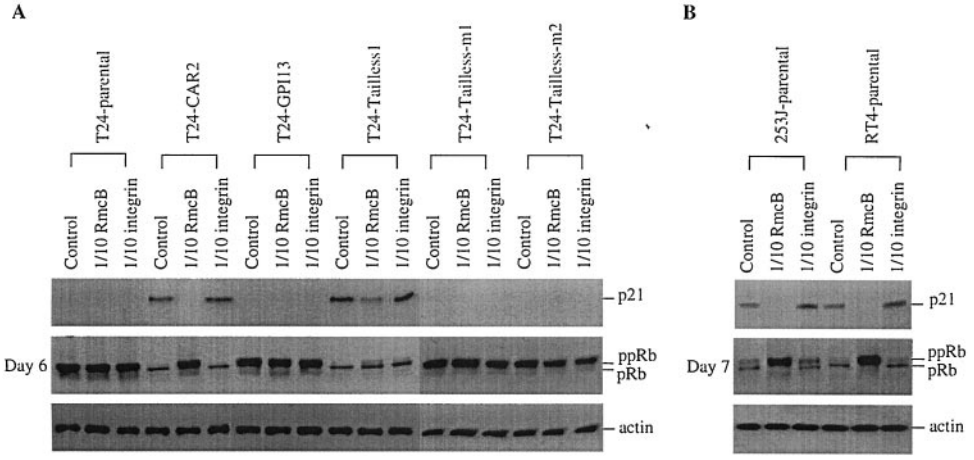

Fig. 7. The effect of CAR antibody on the expression of p21 and Rb protein in bladder cancer cells. Cells were incubated with either CAR antibody or control antibody. At the indicated time, cell lysates from T24 sublines (*A*) or 253J and RT4 sublines (*B*) were subjected to Western blot analysis probed with anti-p21, Rb, and β-actin antibodies. *ppRb,* hyperphosphorylated form of Rb; *pRb,* hypophosphorylated form.

of CAR may be a potential site for posttranslational lipid modification such as farnesylation, prenylation, and palmitoylation (23–26). It is known that posttranslational lipid modification plays a critical role in protein-protein interaction and protein-membrane association, which is a key mechanism in modulating signal transduction. Therefore, CAR may associate with effector protein(s) to elicit the growth-inhibitory signal cascade.

In this study, we also delineated the underlying mechanism elicited by CAR as a potent growth inhibitor. We examined the expression of two key cell cycle regulators (p21 and Rb) that are involved in bladder cancer progression (11). In general, elevated levels of p21 protein result in the accumulation of hypophosphorylated Rb, which leads to G_1 cell cycle arrest and/or apoptosis (27, 28). Cell lines with high CAR levels and slow growth showed high levels of p21 protein (Fig. 4). Conversely, cells with low CAR levels or Tailless-m and GPI clones without essential parts of cytoplasmic domain had rapid growth showed low p21 protein. Moreover, we found that decreasing endogenous CAR levels in both 253J and RT4 cells by antisense strategy led to fast cell growth accompanied with p21 decline and increased inactive Rb protein (Fig. 4, *C* and *D*). These data suggest that CAR may act as a key mediator for the contact inhibition occurring among normal cells but absent in cancer cells.

We examined the relationship between the adhesion activity of CAR and its capacity to inhibit growth of bladder cancer. A CAR-specific antibody inhibited aggregation of all CAR-positive cell lines (Fig. 5) and restored the growth rate in cell lines expressing full-length CAR as well as CAR containing the "functional" cytoplasmic domain (Table 2 and Fig. 6). CAR antibody-alleviated growth suppression of T24-CAR, T24-Tailless, 253J, and RT4 cells was further evidenced by the decreased p21 protein and increased Rb phosphorylation levels (Fig. 7).

We showed previously that C-CAM1 can still inhibit tumor growth without the first immunoglobulin domain (13, 29) that is required for its homophilic interaction (30). In contrast, now it appears that CAR-mediated adhesion may be critical for initiating a growth-inhibitory signal cascade. However, intercellular adhesion elicited by CAR is essential, but not sufficient, for its growth-inhibitory activity because the intracellular domain of CAR is needed for recruiting effector protein(s) that modulates cell cycle regulators inside the nucleus of bladder cancer cells. Therefore, a search for any downstream effector(s) is warranted.

Our findings indicate that increased expression of CAR protein can enhance viral uptake and inhibit tumor growth by increasing intercellular contact. This dual function indicates that CAR has significant biological and therapeutic potential to enhance therapy for human bladder cancer. Moreover, our findings indicate that CAR is not just a viral receptor, and it can elicit a negative signal cascade to modulate cell cycle regulators inside the nucleus of bladder cancer cells. These results can be integrated to formulate a new strategy for bladder cancer therapy.

ACKNOWLEDGMENTS

We thank Andrew Webb for editing the manuscript.

REFERENCES

1. Philipson, L., Lonberg-Holm, K., and Pettersson, U. Virus-receptor interaction in an adenovirus system. J. Virol., *2:* 1064–1075, 1968.
2. Bergelson, J. M., Cunningham, J. A., Drouguett, G., Kurt-Joned, E. A., Krithivas, A., Hong, J. S., Horwitz, M. S., Crowell, R. L., and Finberg, R. W. Isolation of a common receptor for coxsackie B viruses and adenoviruses 2 and 5. Science (Wash. DC), *275:* 1320–1323, 1997.
3. Tomko, R., P., Xu, R., and Philipson, L. HCAR and MCAR: the human and mouse cellular receptors for subgroup C adenoviruses and group B coxsackieviruses. Proc. Natl. Acad. Sci. USA, *94:* 3352–3356, 1997.
4. van Raaij, M. J., Chouin, E., van der Zandt, H., Bergelson, J. M., and Cusack, S. Dimeric structure of the coxsackievirus and adenovirus receptor D1 domain at 1.7 Å resolution. Structure, *8:* 1147–1155, 2000.
5. Li, Y., Pong, R-C., Bergelson, J. M., Hall, M. C., Sagalowsky, A. I., Tseng, C-P., Wang, Z., and Hsieh, J. T. Loss of adenoviral receptor expression in human bladder cancer cells: a potential impact on the efficacy of gene therapy. Cancer Res., *59:* 325–330, 1999.
6. Wang, X., and Bergelson, J. M. Coxsackievirus and adenovirus receptor cytoplasmic and transmembrane domains are not essential for coxsackievirus and adenovirus infection. J. Virol., *73:* 2559–2562, 1999.
7. Okegawa, T., Li, Y., Pong, R-C., Bergelson, J. M., Zhou, J., and Hsieh, J. T. The dual impact of coxsackie and adenovirus receptor (CAR) expression on human prostate cancer gene therapy. Cancer Res., *60:* 5031–5036, 2000.
8. Sambrook, J., Fritsch, E. F., and Maniatis, T. Molecular Cloning: A Laboratory Manual, Ed. 2, pp. 16.66–16.67. Cold Spring Harbor, NY: Cold Spring Harbor Laboratory, 1989.
9. Tseng, C-P., Ely, B., Pong, R-C., Li, Y., and Hsieh, J. T. Regulation of the *DOC-2* gene during castration-induced rat ventral prostate degeneration and its growth inhibitory function in human prostatic carcinoma cells. Endocrinology, *139:* 3542–3553, 1998.
10. Gleave, M. E., Hsieh, J. T., Gao, C. A., von Eschenbach, A. C., and Chung, L. W. K. Acceleration of human prostate cancer growth *in vivo* by factors produced by prostate and bone fibroblasts. Cancer Res., *51:* 3753–3761, 1991.
11. Hall, M. C., Li, Y., Pong, R-C., Ely, B., Sagalowsky, A. I., and Hsieh, J. T. The growth inhibitory effect of p21 adenovirus on human bladder cancer cells. J. Urol., *163:* 1033–1038, 2000.
12. Hsieh, J. T., Luo, W., Song, W., Wang, Y., Kleinerman, D., Van, N. T., and Lin, S-H. Tumor suppressive role of an androgen-regulated epithelial cell adhesion molecule (C-CAM) in prostate carcinoma cell revealed by sense and antisense approaches. Cancer Res., *55:* 190–197, 1995.
13. Hsieh, J. T., Earley, K., Pong, R-C., Wang, Y., Van, N., T., and Lin, S-H. Structural analysis of the C-CAM1 molecule for its tumor suppression function in human prostate cancer. Prostate, *41:* 31–38, 1999.
14. Kleinerman, D., Troncoso, P., Lin S-H., Pisters, L. L., Sherwood, E. R., Brooks, T., von Eschenbach, A. C., and Hsieh, J. T. Consistent expression of an epithelial cell adhesion molecule (C-CAM) during human prostate development and loss of expres-

sion in prostate cancer: implication as a tumor suppressor. Cancer Res., *55:* 1215–1220, 1995.
15. Kleinerman, D., Diney, C., Zhang, W. W., Lin S-H., Van, N. T., and Hsieh, J. T. Suppression of human bladder cancer growth by increased expression of *C-CAM1* gene in an orthotopic model. Cancer Res., *56:* 3431–3435, 1996.
16. Graham, F., and Prevec, L. Manipulation of adenovirus vector. *In:* E. J. Murray (ed.), Methods in Molecular Biology: Gene Transfer and Expression Protocol, Vol. 7, pp. 109–128. Clifton, NJ: Humana Press, 1991.
17. Stevenson, S. C., Rollence, M., White, B., Weaver, L., and McClelland, A. Human adenovirus serotypes 3 and 5 bind to two different cellular receptors via the fiber head domain. J. Virol., *69:* 2850–2857, 1995.
18. Freimuth, P. A human cell line selected for resistance to adenovirus infection has reduced levels of the virus receptor. J. Virol., *70:* 4081–4085, 1996.
19. Hemmi, S., Geertsen, R., Mezzacasa, A., Peter, I., and Dummer, R. The presence of human coxsackievirus and adenovirus receptor is associated with efficient adenovirus-mediated transgene expression in human melanoma cell cultures. Gene Ther., *9:* 2363–2373, 1998.
20. Miller, C., R., Buchsbaum, D., J., Reynolds, P. N., Douglas, J. T., Gillespie, G. Y., Mayo, M. S., Raben, D., and Curiel, D. T. Differential susceptibility of primary and established human glioma cells to adenovirus infection: targeting via the epidermal growth factor receptor achieves fiber receptor-independent gene transfer. Cancer Res., *58:* 5738–5748, 1998.
21. Asaoka, K., Tada, M., Sawamura, Y., Ikeda, J., and Abe, H. Dependence of efficient adenoviral gene delivery in malignant glioma cells on the expression levels of the coxsackievirus and adenovirus receptor. J. Neurosurg., *92:* 1002–1008, 2000.
22. Honda, T., Saitoh, H., Masuko, M., Katagiri-abe, T., Tomonaga, K., Kozakai, I., Kobayashi, K., Kumanishi, T., Watanabe, Y. G., Odani, S., and Kuwana, R. The coxsackievirus-adenovirus receptor protein as a cell adhesion molecule in the developing mouse brain. Mol. Brain Res., *77:* 19–28, 2000.
23. Gibbs, J. B., Oliff, A., and Kohl, N. E. Farnesyltransferase inhibitors. Ras research yields a potential cancer therapeutic. Cell, *77:* 175–178, 1994.
24. Zhang, F. L., and Casey, P. J. Protein prenylation: molecular mechanisms and functional consequences. Annu. Rev. Biochem., *65:* 214–269, 1996.
25. Milligan, G., Parenti, M., and Magee, A. I. The dynamic role of palmitoylation in signal transduction. Trends Biochem. Sci., *20:* 181–187, 1995.
26. Sinensky, M. Recent advances in the study of prenylated proteins. Biochim. Biophys. Acta, *1484:* 93–106, 2000.
27. Zhao, X., Gschwents, J., E., Powell, T., Foster, R. G., Day, K. C., and Day, M. L. Retinoblastoma protein-dependent growth signal conflict and caspase activity are required for protein kinase C-signaled apoptosis of prostate epithelial cells. J. Biol. Chem., *272:* 22751–22757, 1997.
28. Blagosklonny, M. V., Prabhu, N. S., and El-deiry, W. S. Defects in p21WAF1/CIP1, Rb, and c-myc signaling in phorbol ester-resistant cancer cells. Cancer Res., *57:* 320–325, 1997.
29. Luo, W., Wood, C. G., Early, K., Hung, M. C., and Lin, S-H. Suppression of tumorigenicity of breast cancer cells by an epithelial cell adhesion molecule (C-CAM1): the adhesion and growth suppression are mediated by different domains. Oncogene, *14:* 1697–1704, 1997.
30. Cheung, P. H., Luo, W., Qiu, Y., Zhang, X., Earley, K., Millirons, P., and Lin, S-H. Structure and function of C-CAM1: the first immunoglobulin domain is required for intercellular interaction. J. Biol. Chem., *268:* 24303–24310, 1993.